POKER

POsitron resonant annihilation into dar**K** matt**ER**

POKER-NOTE-23-12
January 29, 2024

Measurement for the e^+ beam purity at the CERN-SPS H8 beamline

P.Bisio, M. Bondí, A. Celentano, A. Marini, L. Marsicano

1 Introduction and motivation

This Note describes the e^+-beam purity measurement for the H8 beamline of the Super Proton Synchrotron (SPS) at CERN. This study was performed in the context of the POKERINO prototype characterization, conducted during a week of measurements in the summer of 2023 at the H8 beamline. Given the many users exploiting this facility, we decided to share this study with the CERN community.

2 The Experimental Setup

The POKERINO calorimeter is a 3x3 matrix of $PbWO_4$ crystals, each with dimensions 2x2x25 cm^3. The scintillation light from each crystal is read by 4 SiPMs, coupled to one of the two 2x2 cm^2 crystal faces with an optical glue. The nine crystals are embedded in a copper structure, connected to an external, water-based cooling system, and inserted in a black, light-tight box. The measurements were performed in the PPE158 experimental area of the H8 line of the Super Proton Synchrotron at CERN. This beamline provided a positron beam with energy ranging from 10 GeV to 120 GeV and an intensity up to 10^4 particles/spill. Figure 1 shows a schematic of the experimental setup. Two upstream plastic scintillators (PMT-1 and PMT 2: 5x5x1.5 cm^3), located along the beamline and separated by about one meter, were used to detect impinging particles. A PMT read each scintillator. The coincidence between the two discriminated signals provided the trigger signal for the DAQ system. POKERINO was installed on a DESY table that allowed us to move the prototype in the plane orthogonal to the beam (X-Y plane in the figure), align POKERINO with the beamline, and change the particle impact point on the detector. POKERINO was mounted on a rotating platform to rotate it in a plane parallel to the ground (Y-Z plane in the figure). The cooling system kept the calorimeter's temperature at 20°C. In addition, three threshold Cherenkov systems (xcet 042474, xcet 042519, xcet 042537), based on helium gas chambers and installed along the line, allowed for a rough identification of the impinging particles' nature. The signal from the two scintillator pads, the nine POKERINO channels and the Cherenkov counters were digitized by flash ADC (CAEN V1725, 250 MHz sampling frequency) and acquired through the DAQ system.

3 Measurements

The presented study aimed to discriminate impinging positrons against other particles contaminating the beam (hadrons and muons). The applied selection is based on the POKERINO calorimetric measurement

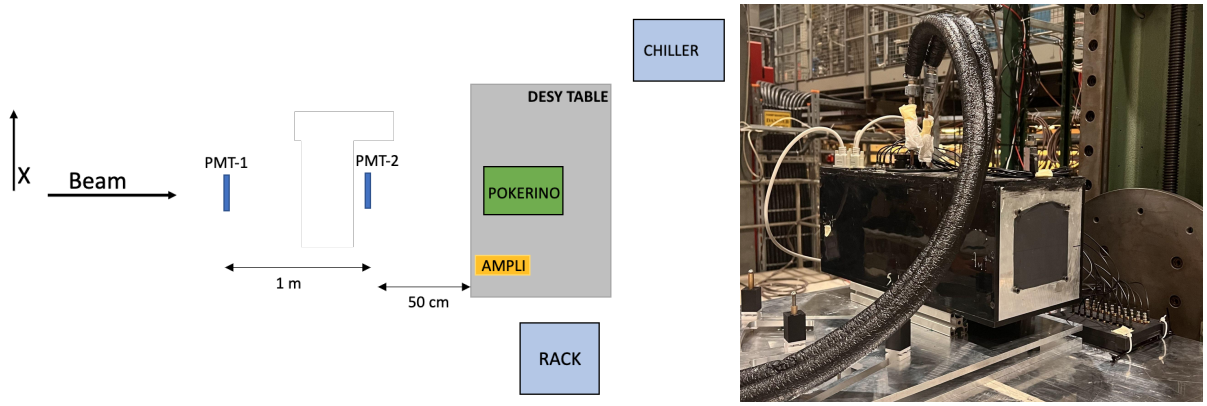

Figure 1: Left: A scheme of the experimental setup used during the described measurements. Right: the image of POKERINO lying on the DESY table in the PPE158 experimental area. The rotating platform is visible under the calorimeter.

and the Cherenkov detector signals. We performed this study by acquiring different runs for different values of beam energy: 10 GeV, 20 GeV, 30 GeV, 40 GeV, 60 GeV, 80 GeV, 100 GeV and 120 GeV. In these runs, the calorimeter was aligned with the beam, and particles impinged on the central crystal of the active $PbWO_4$ matrix. In addition, some runs were performed with the vertical momentum slits (042132 and 042407) at a different aperture than the nominal one ($\pm$ 40 mm), allowing us to study the effects of collimators on the beam-purity measurement.

We set the pressure of the Cherenkov detectors to obtain a refractive index for Helium: $n_{set} = (n_\pi - 1) \times 0.9 + 1$; in this formula, $n_\pi = 1/\beta_\pi$ represents the threshold value at which pions start to emit Cherenkov radiation. Pions did not emit Cherenkov light in these conditions, while positrons did. In principle, muons could generate radiation, but their high-penetrating behaviour resulted in a clear experimental signature, allowing us to identify them correctly as contaminating particles.

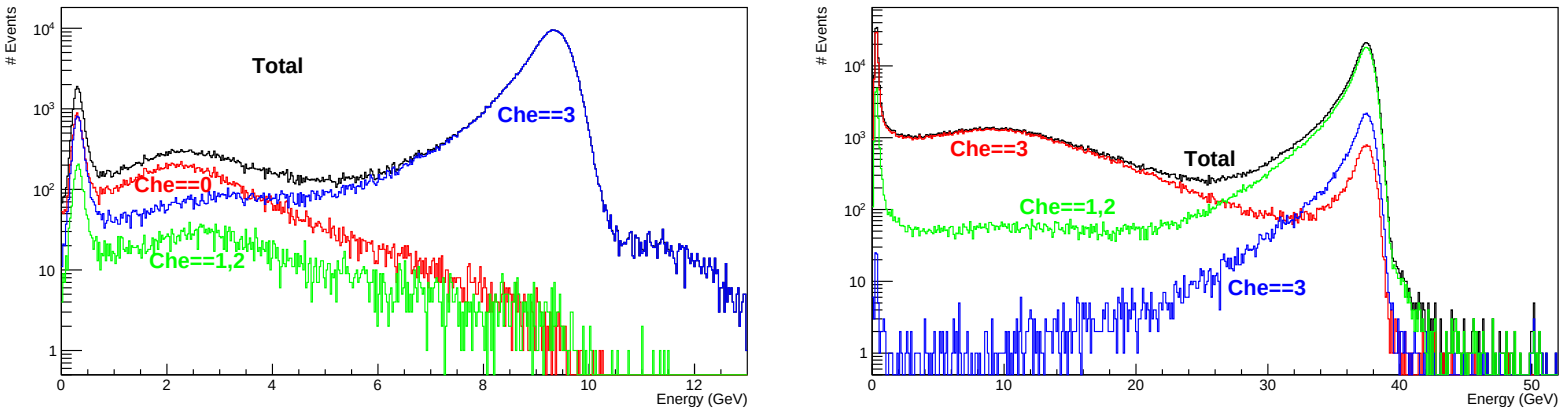

Figure 2: The energy spectrum measured by POKERINO for the 10 GeV (left) and 40 GeV (right) positron beam. The three coloured curves correspond to events with no signal from the Cherenkov counters (in red), those in which it was present in one or two (in green), and those in which all three counters detected the impinging particle (in blue).

Looking at the POKERINO energy spectrum (Fig. 2) for each beam configuration, three regions can be distinguished. The particles acting as MIP (μ and π passing through POKERINO without any hard interaction) populate the $\sim$ 300 MeV peak. A second peak is observed for $E \simeq E_{Beam}$. This is due to positrons that generate an electromagnetic shower, completely absorbed by the calorimeter. In the intermediate region, the spectrum is mainly populated by events where the incident pion produces a hadronic shower, not completely contained in POKERINO. Cherenkov counters measurements confirm these observations. Figure 2, left panel, shows the energy spectrum for the 10 GeV positron beam. This spectrum was divided into three regions: events with no signal in the Cherenkov counters (in red), those in which it was present in one or two (in green), and those in which all three counters detected the

impinging particle (in blue). The full-energy deposition peak is uniquely populated by events belonging to the third category, motivating the assumption that positrons were impinging on POKERINO. The spectrum central region is mainly occupied by events in which no Cherenkov light was detected, indicating that pions generated them, while both pion and muon events populate the low-energy region. On the other hand, by increasing the beam energy, the number of Cherenkov photons emitted by the impinging positrons decreases, not activating the Cherenkov detector. Consequently, Fig. 2 on the right, relative to the 40 GeV positron beam, exhibits full-energy deposition events in which no Cherenkov light was detected.

In light of these observations, we identified events in which POKERINO detected at least $f = 65\%$ of the nominal beam energy as positron events. Thus, the beam purity was computed as the ratio between positron events and the total event number. The f threshold was arbitrarily chosen in the range between the positron and pion energy distribution. In this region, the spectra are quite flat and modifying the selection does not dramatically affect the beam purity measurement. In particular, the systematic uncertainty of the measurement was evaluated as the difference between beam purity measurement assuming $f = 55\%$ with those computed defining $f = 75\%$. In addition, for low-energy runs (10 GeV, 20 GeV, 30 GeV), the positron events selection also required at least a signal from a Cherenkov counter. Adding this cut does not significantly affect the result that is dominated by the definition of f. This last observation indicates that we can rely on the purity measurement for high-energy beams, even if the Cherenkov detector could not provide measurements useful for the positron events selection.

4 Results

The results of this study are summarized in Tab. 1 and Fig. 3. During the first two runs performed with $E_{Beam} = 40$ GeV, the vertical momentum slits (042132 and 042407) were in the nominal position ($\pm$ 40 mm). In the following two runs, collimators were closed to $\pm$15 mm, decreasing the beam purity. The same behaviour is observed in the 100 GeV data in which we progressively closed the slits (see Tab. 1). This observation suggests that the positron beam profile is broader than the contaminating particles one. Thus, closing the collimators, we removed the less-focused positrons (carrying a momentum slightly different from the nominal one), reducing the beam purity. Moreover, between run 1608 and run 1619, the T4 target was changed to a longer one, significantly increasing the beam purity for the second half of our studies. In conclusion, in each run pair that was acquired under the same experimental conditions the beam purity measurements are compatible, suggesting that this observable uniquely depends on the beamline configuration.

5 Acknowledgments

The authors warmly thank E. Tixi for the invaluable support during the POKERINO detector installation and commissioning. This result is part of a project that has received funding from the European Research Council (ERC) under the European Union's Horizon 2020 research and innovation programme, Grant agreement No. 947715 (POKER).

Run N	Beam Energy	Collimators Position	T4 Target	e^+ Beam Purity
1511	10 GeV	±40 mm	Type-S	0.85 ± 0.05
1521	10 GeV	±40 mm	Type-S	0.86 ± 0.05
1524	20 GeV	±40 mm	Type-S	0.66 ± 0.04
1538	30 GeV	±40 mm	Type-S	0.64 ± 0.03
1551	30 GeV	±40 mm	Type-S	0.64 ± 0.03
1555	40 GeV	±40 mm	Type-S	0.57 ± 0.03
1576	40 GeV	±40 mm	Type-S	0.57 ± 0.03
1579	40 GeV	±15 mm	Type-S	0.42 ± 0.03
1581	40 GeV	±15 mm	Type-S	0.42 ± 0.03
1592	60 GeV	±40 mm	Type-S	0.50 ± 0.03
1608	80 GeV	±40 mm	Type-S	0.51 ± 0.03
1619	80 GeV	±40 mm	Type-L	0.73 ± 0.03
1624	100 GeV	±40 mm	Type-L	0.74 ± 0.03
1636	100 GeV	±40 mm	Type-L	0.74 ± 0.04
1637	100 GeV	±30 mm	Type-L	0.71 ± 0.04
1638	100 GeV	±20 mm	Type-L	0.65 ± 0.03
1639	100 GeV	±15 mm	Type-L	0.60 ± 0.03
1641	100 GeV	±15 mm	Type-L	0.60 ± 0.03
1650	60 GeV	±40 mm	Type-L	0.72 ± 0.04
1655	120 GeV	±40 mm	Type-L	0.15 ± 0.01
1664	120 GeV	±40 mm	Type-L	0.15 ± 0.01

Table 1: The e^+ beam purity measurement for different runs. The beam energy and the aperture of vertical momentum slits 042132 and 042407 are also reported. Between run 1608 and run 1619, the T4 target (Type-S) was substituted with a longer one (Type-L). Read the text for details.

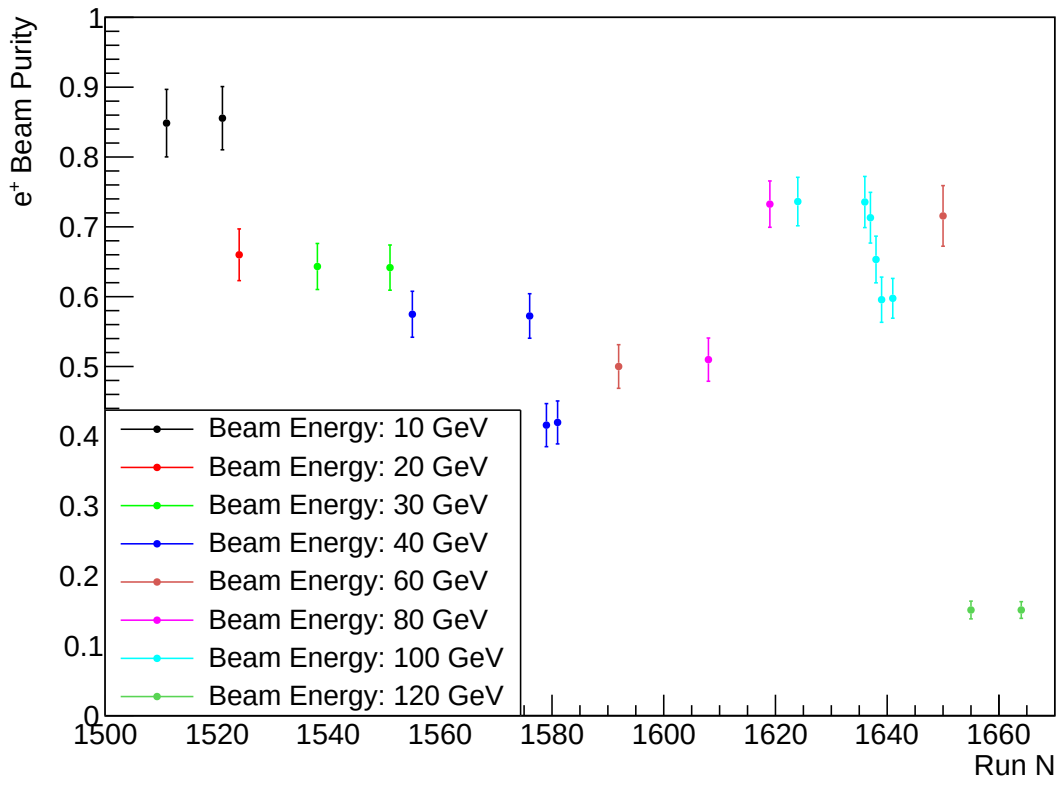

Figure 3: The e^+ beam purity measurement for different runs. The different beam energies are highlighted through colours, described in the legend. Read the text for details.